Sensitivity Improvement in NQR Based Detection Methods

M. Steinbauer, J. Seginák, and P. Dohnal
Department of Theoretical and Experimental Electrical Engineering
Brno University of Technology, Technická 12, Brno 616 00, Czech Republic

Abstract— This article presents an approach to sensitivity improvement in a detection method based on nuclear quadrupole resonance (NQR); this technique is widely applied in, for example, the detection of explosives. We have an experimental pulsed NQR apparatus equipped with a 250 W pulse power rf amplifier with the working frequency range from 0.5 to approximately 50 MHz. This range can be employed in detecting the isotopes ^{14}N and ^{35}Cl. The article will describe certain improvements in the circuitry of the NQR system proposed by the authors and then experimentally verified on the existing system. These modifications lead to an increased signal-to-noise ratio (SNR), thus also increasing the sensitivity of the system during the detection of substances. The main improvements are in the rf blocking circuit, which prevents the power rf pulse from reaching the preamplifier of the receiver. In this position, some impedance transformers with switched coils have been tested. The appropriate quenching circuit further reduces the penetration of the excitation pulse to this sensitive preamplifier and thus shortens the recovery time.

1. INTRODUCTION

The principles of NQR spectroscopy can be found in [1, 2]. The experimental NQR spectrometer installed in our laboratory uses a SpinCore radioprocessor for signals in the range of 0–100 MHz. The board has two analog I/O channels and four digital outputs. The sampling rate is up to 75 MSPS with 14-bit resolution; the converter utilizes quadrature detection. The DDFS generator provides a signal with the resolution of 14 bits at a frequency of up to 300 MSPS with the baseband bandwidth of 10 MHz. The best achievable time resolution of the radioprocessor is 13.3 ns.

The block diagram of the spectrometer is shown in Figure 1. The 250 W rf amplifier is keyed to reduce the noise in the phase of FID acquisition. An active damping circuit is employed to shorten the time between the excitation and signal acquisition due to the decay of the LC probe.

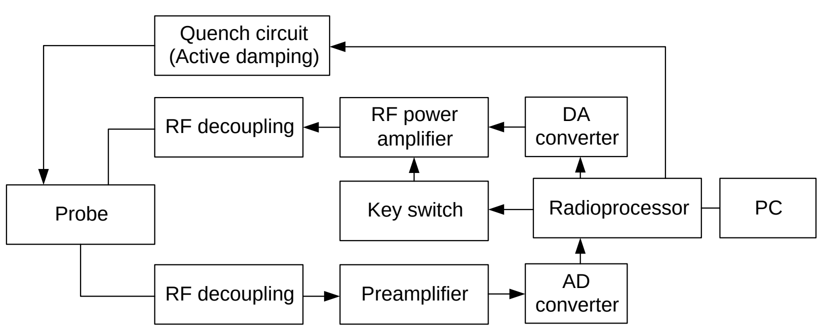

Figure 1: The block diagram of the NQR experimental spectrometer with a radioprocessor.

2. RF DECOUPLING

We decided to compare the properties of two different concepts of rf decoupling on our experimental NQR system.

2.1. LC Filter

To separate the sensitive input of the rf preamplifier from the power circuitry, an LC filter is normally used; this filter is often formed as π-match, see Figure 2 or source [3]. During the operation of the power amplifier, which two pairs of antiparallel diodes will open, and the filter behaves like an impedance divider with high attenuation (L_1 impedance vs input impedance of the preamplifier including protection diodes). At the time of the FID signal acquisition, this circuit acts as a low-pass frequency filter, limiting the undesirable spectral components and thus improving the SNR. The filter is tuned to the desired center frequency with the declared bandwidth.

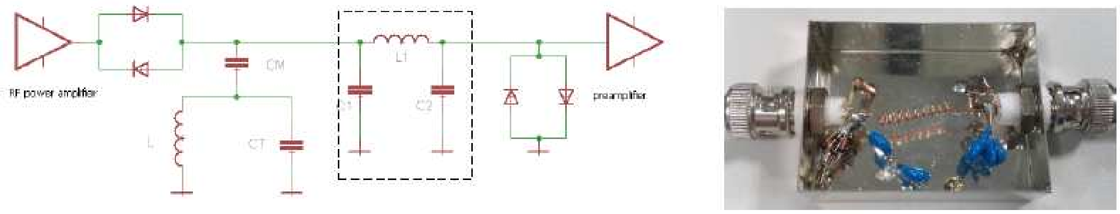

(a) (b)

Figure 2: (a) The basic diagram of the parallel resonance NQR detector (L is the coil of the probe). (b) The π-match implementation for 28 MHz center frequency.

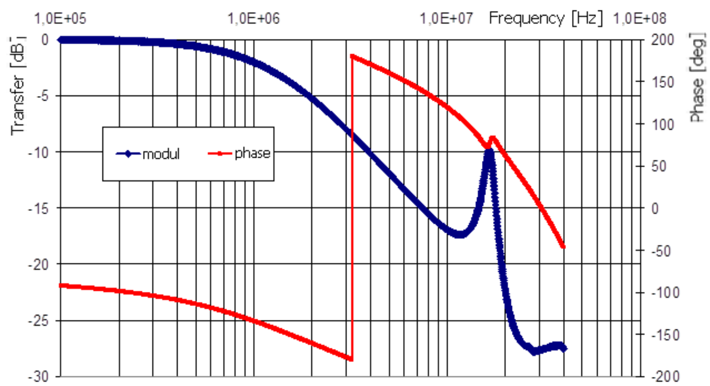

Figure 3: The measured transmission characteristics of the π-match circuit from Figure 2.

One of the filters used in our experimental NQR spectrometer is a π-match with the cut-off frequency of 28 MHz. In the passband, it has an acceptable insertion loss of about 7 dB. Since this filter is narrowband, it is advisable to have one of these circuits for each frequency band and change it when tuning to another spectral region. In NQR detection, we can universally employ π-match filters with the central frequencies of 1; 3.5; 5; 12; 28 MHz or higher.

2.2. Impedance Transformer

Another solution how to isolate the rf preamplifier from the power amplifier consists in the use of an impedance transformer (Figure 4); this approach is described in reference [4]. If no current flows through the lower winding (which is disconnected), the upper winding of the transformer acts as an inductor and exhibits high impedance for the rf signal. If the transistor is turned on, the switching diodes open and short-circuit the lower winding of the transformer; then, the upper coil also exhibits low impedance, and the rf signal passes to the preamplifier.

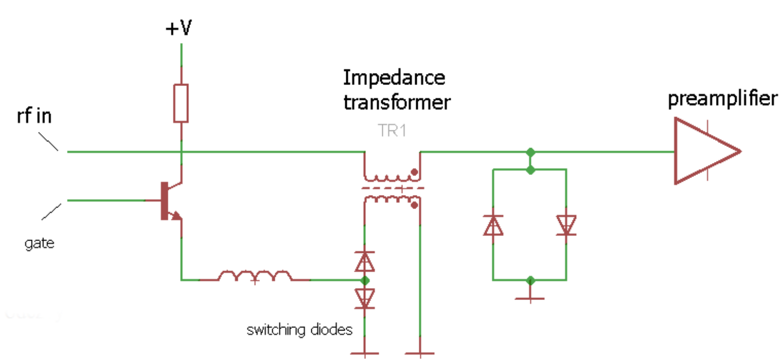

Figure 4: The decoupling of the rf preamplifier pulses performed by the transformer.

3. RESULTS AND DISCUSSION

We designed and experimentally built the circuit according to Figure 4. The transformer 1 : 1 was wound bifilarly from a R174 coaxial cable having the characteristic impedance of 50 Ω. In terms of shielding, the outer wire of the coaxial cable is used as the switched winding and the internal wire as the rf winding. A very important parameter consists in the core material, which must correspond to the particular frequency and have high permeability. The number and distribution of the threads is especially significant with respect to the parasitic capacity and influences the behavior of the transformer. Some of the cores have been tested: the T106-2 with 7 turns (A), the T5020 with 21 turns (B) based on the CF195 material, and the FT140-43 with 30 turns (C).

First, the properties of the actual transformers were measured via simple short-circuiting and opening of the primary winding. The measured results for the transformers (A) and (C) are shown in the graphs in Figures 5 and 6.

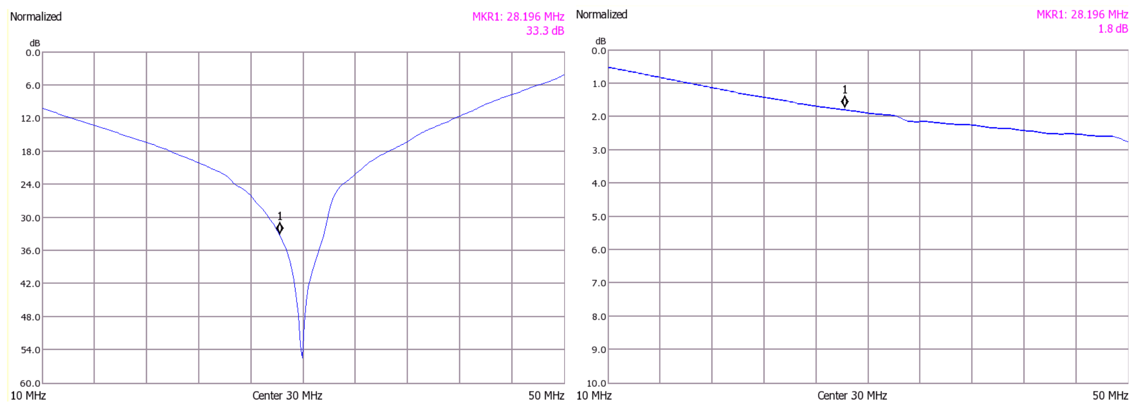

(a) (b)

Figure 5: The attenuation of the impedance transformer (A) with the (a) primary winding opened and (b) short-circuited; the attenuation achieves up to 54 dB at 30 MHz, while the insertion loss is 1.8 dB.

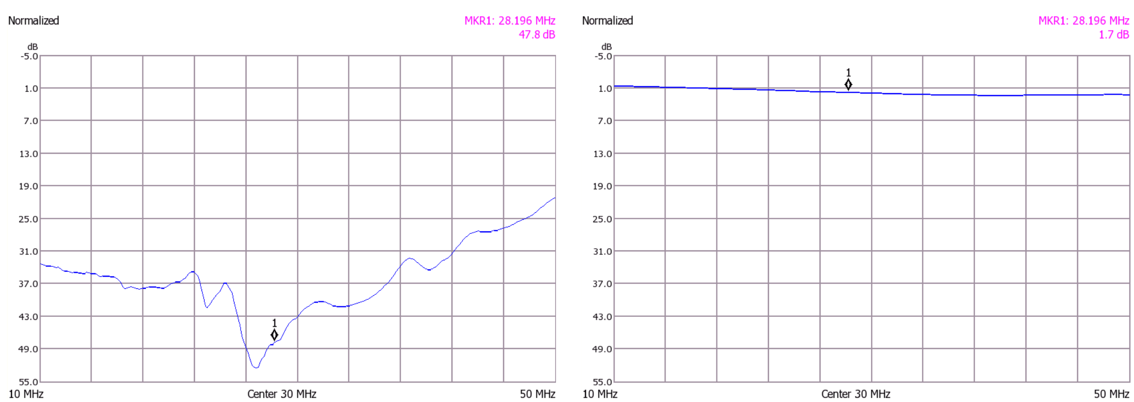

(a) (b)

Figure 6: The attenuation of the impedance transformer (C) with the (a) primary winding opened and (b) short-circuited; the attenuation achieves up to 47.8 dB at 28.1 MHz, while the insertion loss is 1.7 dB.

The transformer (C) was used for the implementation of the circuit according to Figure 7. During the experiments, it was proved that the attenuation of the circuit decreases with the increasing power of the rf signal. This fact is mainly caused by the parasitic capacitance of the diodes in the circuit switch. High-frequency current is transformed to the primary winding and flows through the parasitic capacitance of the diodes; this lowered impedance of the primary winding is then transformed into the secondary one, thus reducing the attenuation. It is therefore appropriate to improve the circuitry and use diodes with minimal parasitic capacitances.

Finally, the response of the entire circuit at the operating frequency of 28 MHz has been tested. The reached switch-off and switch-on times are shown in the oscilloscope images in Figure 7. Here,

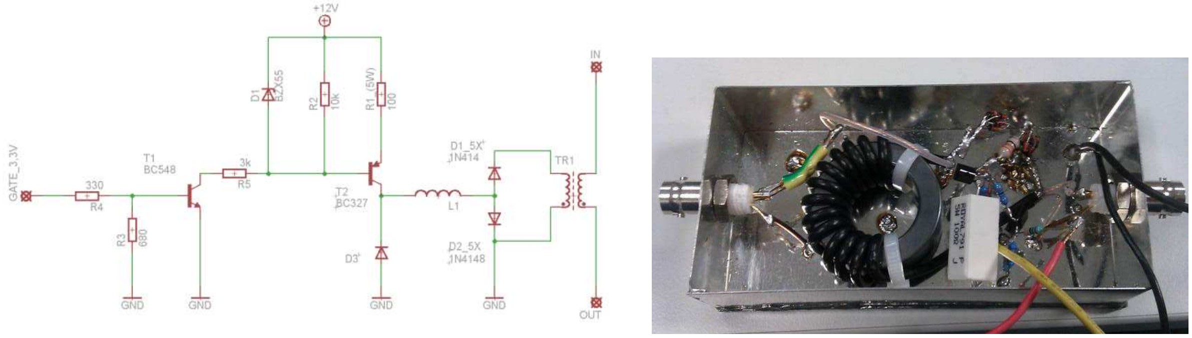

Figure 7: The circuit diagram and photograph of the implemented switch circuit with the impedance transformer.

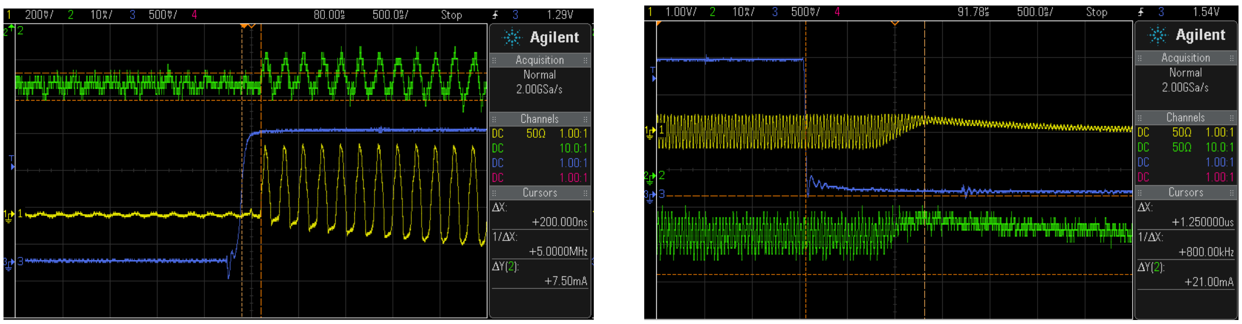

Figure 8: The measured voltage and current waveforms during the transition in the circuit from Figure 7.

the blue curve indicates the keying pulse from the radioprocessor, the yellow curve represents the voltage on the $50\,\Omega$ load, and the green curve represents the current flowing through the windings of the transformer. It is obvious from these oscillograms that the delay between the keying pulse and the current flowing through the transformer is about 200 ns when switching on and approximately 1.25 µs when switching off.

4. CONCLUSION

The implementation of the above-described decoupling circuit reduces the attenuation of the measured FID signal and also shortens the dead time between the sample excitation with an rf pulse and the beginning of the signal acquisition.

The planned sensitivity improvement will be based on the suppression of false signals interchangeable with the FID response; such signals are caused by external rf sources. This could be performed either by a differential method with a reference external antenna or via a switched magnetic field in the sample. The latter option results in the loss of NQR signals in the sample when a magnetic field is applied, and therefore differential measurement with and without a static magnetic field affecting the sample can dramatically highlight the NQR peaks in the spectrum of the detected signal.

ACKNOWLEDGMENT

The presented activities were supported by the project No. FEKT-S-14-2545/2014, Brno University of Technology internal science fund. Further, the research utilized financial assistance from the project No. CZ.1.07.2.3.00.20.0175 within the Education for Competitiveness Operative Programme.

REFERENCES

1. Suits, B. H., "Nuclear quadrupole resonance spectroscopy," *Handbook of Applied Solid State Spectroscopy*, D. R. Vij, Springer, Physics Department, Michigan Technological University, Houston, USA, Jul. 2006, ISBN-10: 0387324976.
2. Sathyanarayana, D. N., *Introduction to Magnetic Resonance Spectroscopy ESR, NMR, NQR*, I.K. International Publishing House, 2009, ISBN-13: 978-9380026251.

3. Hiblot, N., B. Cordier, M. Ferrari, A. Retournard, D. Grandclaude, J. Bedet, S. Leclerc, and D. Canet, "A fully homemade ^{14}N quadrupole resonance spectrometer," *Comptes Rendus Chimie*, Vol. 11, 568–579, Methodologie RMN, Nancy-Universite, Universite Henri-Poincare, France, 2008.
4. Ostafin, M. and B. Nogaj, "^{14}N-NQR based device for detection of explosives in landmines," *Measurement*, Vol. 40, No. 1, 43–54, Elsevier, Department of Physics, Adam Mickiewicz University of Poznan, Umultowska 85, Poznan 61-614, Poland, 2007.